Thermoelectricity in Confined Liquid Electrolytes

Mathias Dietzel* and Steffen Hardt
Institute for Nano- and Microfluidics, Center of Smart Interfaces, TU Darmstadt, Alarich-Weiss-Straße 10, D-64287 Darmstadt, Germany
(Received 30 July 2015; published 2 June 2016)

The electric field in an extended phase of a liquid electrolyte exposed to a temperature gradient is attributed to different thermophoretic mobilities of the ion species. As shown herein, such Soret-type ion thermodiffusion is not required to induce thermoelectricity even in the simplest electrolyte if it is confined between charged walls. The space charge of the electric double layer leads to selective ion diffusion driven by a temperature-dependent electrophoretic ion mobility, which—for narrow channels—may cause thermovoltages larger in magnitude than for the classical Soret equilibrium.

DOI: 10.1103/PhysRevLett.116.225901

The Seebeck effect describes the generation of a thermoelectric potential when a conductor is exposed to a temperature gradient $\boldsymbol{\nabla} T$ [1]. Thermoelectricity and its related effects are the cornerstones of key technologies for temperature measurements [2], refrigeration, and recovery of waste heat [3–5], and have gained renewed interest within the realm of nanoscale transport processes [6]. While the charge carriers in the conduction band of semiconductors may generate a thermoelectric voltage without exhibiting a thermophoretic mobility [7], thermoelectricity in an extended (i.e., electroneutral) phase of a liquid electrolyte is based on thermophoresis of the dissolved ions species k [8]. Their number concentrations n_k align with $\boldsymbol{\nabla} T$ such that the ion fluxes driven by Fickian diffusion and thermophoresis balance each other. The overall salt concentration n is then given by [9]

$$\frac{\boldsymbol{\nabla} n}{n} = -\Pi \frac{\boldsymbol{\nabla} T}{T}. \tag{1}$$

Herein, to highlight the key effects, the discussion is focused on symmetric electrolytes of valence ν ($k = +$ for the cation and $k = -$ for the anion), for which electroneutrality implies $n_+ = n_- = n$. Consequently, the effective Soret coefficient simplifies to read $\Pi = (Q_+ + Q_-)/(2k_B T)$. The Boltzmann constant is denoted by k_B, and the thermophoretic behavior of the ions is quantified in terms of the heats of transport Q_k. For such simple electrolytes, the thermocell electric field is given by [9]

$$\boldsymbol{E}_Q^{(\infty)} = \frac{\Delta Q}{2e\nu} \frac{\boldsymbol{\nabla} T}{T}, \tag{2}$$

i.e., it is solely generated by the difference in the thermophoretic mobilities of the ions expressed by $\Delta Q = Q_+ - Q_-$. The elementary charge is denoted by e. Equations (1) and (2) define the classical Soret equilibrium derived under the assumptions of vanishing flux densities, the absence of an advective velocity u, and electroneutrality throughout the domain.

Electroneutrality holds only for the bulk phase, where the influence of wall charges is negligibly small. Nevertheless, the relatively few theoretical investigations of the thermal membrane potential of electrolytes in charged pores commonly rely on the phenomenological theory of nonequilibrium thermodynamics and averaged transport numbers, neither explicitly resolving the ion distribution inside the pore, nor specifying the surface charge density, nor the pore size [10–13]. While numerous works discuss isothermal transport processes in charged nanochannels [14], practically no investigations are available addressing these interwoven issues in detail if the temperature is not constant. Electrolyte-filled nanopores or nanochannels with a temperature gradient play a key role for various phenomena. For instance, they are essential for the mechanisms by which organisms use ion channels to sense temperature [15–17]. In addition, the nonisothermal ion transport in porous membranes is a promising candidate for the development of efficient thermoelectric energy conversion techniques [18,19]. The purpose of this Letter is to analyze the nonadvective transport phenomena occurring in a slit nanochannel with charged walls and filled with an electrolyte under application of a temperature gradient along the channel. As will be shown, the presence of an electric double layer (EDL) alters the Soret voltage given by (2), but also induces an additional thermoelectric voltage due to the temperature-dependent electrophoretic ion mobility alone, without relying on the intrinsic Soret effect quantified by the parameters Q_k. To the best of our knowledge, such a mechanism has never been explicitly described before. Thermoosmotic effects arising from the mechanical imbalance of the nonisothermal ion cloud of the EDL will be disregarded; i.e., the momentum equations are not solved for. In preliminary, so far unpublished work, they were found to be weak compared to the phenomena discussed herein.

Figure 1 depicts a schematic of the investigated system. The wall temperature of a long slit channel of half-width h filled with a dilute electrolyte uniformly increases by ΔT

 © 2016 American Physical Society

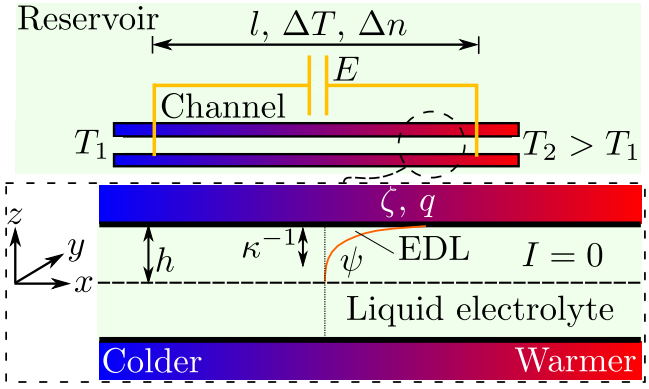

FIG. 1. Sketch of a slit channel of half-width h, submerged in an extended, nonisothermal phase of an aqueous electrolyte. A temperature difference $\Delta T \leq T_2 - T_1$ is present at the channel walls over a length l, leading to an induced thermoelectric field E, and to a gradient in salt concentration $\Delta n/l$. The channel wall carries an electric surface charge density q or is kept at a constant ζ potential. The wall charge is screened by ions in the electric double layer (EDL) of thickness κ^{-1} with an internal potential ψ. The total electric current I over the channel cross section vanishes.

over a length of l. The analysis of this Letter is based on the leading-order contribution of an asymptotic expansion in the small parameter $A = h/l$, while the dimensionless axial gradients of any quantity $n_k, T, \ldots$ are assumed to be small. As verified in the Supplemental Material ([20], Sec. 1), advection, viscous dissipation, and Joule heating can be neglected in the energy equation. Hence, to first order in A, the temperature gradient in the interior of the channel is given by $\boldsymbol{\nabla} T = (\Delta T/l, 0)$, even if the thermal conductivity of the electrolyte varies with temperature. With D_k being the Fickian diffusion coefficients of the ion species, the ionic Péclet numbers, $\mathrm{Pe}_k = ul/D_k$, are negligibly small in the present system ([20], Sec. 1). The Nernst-Planck equations (NPE), governing the ion concentrations, simplify to $\boldsymbol{\nabla} \cdot \boldsymbol{j}_k = 0$ ([20], Sec. 2), with

$$-\boldsymbol{j}_k = D_k \boldsymbol{\nabla} n_k + n_k \mu_k \boldsymbol{\nabla} T + e\nu_k n_k \omega_k \boldsymbol{\nabla}\phi \tag{3}$$

being the ion flux densities, where $\mu_k \equiv D_k Q_k/(k_B T^2)$ and $\boldsymbol{j}_k = (j_{k,x}, j_{k,z})$. The overall electric field $\boldsymbol{\nabla}\phi = \boldsymbol{\nabla}\psi - \boldsymbol{E}$ is the sum of the EDL field $\boldsymbol{\nabla}\psi$, fulfilling the Poisson equation, and an induced electric field $\boldsymbol{E}$ with vanishing associated charge density (source free) [33]. For $A^2 \ll 1$, the Laplace equation and the symmetry condition at the channel center imply that $\boldsymbol{E} \approx (E, 0)$ ([20], Sec. 3). The electrophoretic ion mobilities are given by the classical Stokes-Einstein relation $\omega_k = D_k/(k_B T)$. To leading order in A of the NPE and again incorporating the symmetry at the channel center, the ion concentrations are determined from (3) by $j_{k,z} = 0$. Together with $\partial_z T \equiv \partial T/\partial z = 0$, one finds that the local ion number concentrations are given by ([20], Sec. 3)

$$n_k = n_{k,0} \exp\left(-\frac{e\nu_k \psi}{k_B T}\right), \tag{4}$$

which resemble the Boltzmann distribution. The local ion concentrations at $\psi = 0$ (electroneutral region) are denoted by $n_{k,0}$, which may be a function of x [34]. For a symmetric electrolyte, $n_{k,0} \equiv n$ for each ion species. Despite its familiar appearance, Eq. (4) is a consequence of the smallness of A and the symmetry along the channel center, rather than of directly imposing thermodynamic equilibrium. Unlike in the conventional Soret equilibrium, $n_+ \neq n_- \neq n$. By inserting (4) in (3), the axial flux densities are given by

$$-\frac{j_{k,x}}{n_k D_k} = d_x \ln(n) + \frac{e\nu_k}{k_B T}\left[-E + \left(\frac{Q_k}{e\nu_k} + \psi\right) d_x \ln(T)\right], \tag{5}$$

where $d_x(.) \equiv d(.)/dx$. For simple salts, the coefficients D_k are very similar to each other. Focusing on the essential effects, identical $D_k \equiv D$ are assumed in the following. However, D does not need to be a constant and may vary with T. Under no external electric load, E is calculated by setting the overall electric current, $I = e\nu \int_0^h (j_{+,x} - j_{-,x}) dz$, to zero. This is equivalent to what is done in studies of thermoelectricity in bulk electrolytes [9]. For the Seebeck coefficient $S \equiv E/d_x T$ one finds ([20], Sec. 4)

$$S = S_Q + S_\psi, \tag{6}$$

where

$$S_Q = \frac{1}{T}\frac{\Delta Q}{2e\nu}\frac{\int_0^h e^{-\Psi} dz - \frac{q}{2e\nu n}}{\int_0^h \cosh(\Psi) dz}, \tag{7}$$

$$S_\psi = \frac{1}{T}\frac{\int_0^h \psi \cosh(\Psi) dz}{\int_0^h \cosh(\Psi) dz}. \tag{8}$$

The surface charge density is denoted by $q = -\epsilon(\partial_z \psi)_{|z=h}$, with ϵ being the (temperature-dependent) dielectric permittivity, while $\Psi \equiv e\nu\psi/(k_B T)$. To derive E and since the functional form of n cannot be determined within the employed approximation scheme, $d_x \ln(n) = d_x n/n$ was expressed by (1). While being accurate for channels with nonoverlapping EDLs, for narrower channels this assumption can be justified by viewing the channel as being submerged in a large, nonisothermal tank and referring to a system in electrochemical equilibrium for every local value of T ([20], Sec. 4). Furthermore, neglecting terms of $O(A^2)$, the Poisson equation $\boldsymbol{\nabla} \cdot (\epsilon \boldsymbol{\nabla}\psi) = -\rho_f$ was used, with $\rho_f = e\nu(n_+ - n_-)$ being the charge density. Note that, to first order in A, the term $\boldsymbol{\nabla}\epsilon \cdot \boldsymbol{\nabla}\psi$ can be neglected in the Poisson equation, even though $\epsilon = \epsilon(T)$.

On the one hand, S_Q defined by (7) expresses the thermoelectric field caused by the Soret-type thermophoretic ion motion under confinement. The presence of an EDL modifies its corresponding bulk value, given in form of the

classical Soret equilibrium by (2), to which Sd_xT reduces for an uncharged or very wide channel. On the other hand, S_Q vanishes even under confinement if the heats of transport of both ion species are identical ($\Delta Q = 0$). However, in that case the overall thermoelectric field does not necessarily vanish but is given by $(S)_{|\Delta Q \equiv 0} = S_\psi$ alone. If $\Delta Q \neq 0$, S_Q and S_ψ are additive. Since advection is completely neglected herein, the latter field does not have a thermoosmotic origin ([20], Sec. 5). Instead, according to (4), the temperature-dependent electrophoretic ion mobility implies axial gradients of n_k within the EDL, which are additive to (1), while the magnitude of the affiliated (Fickian) diffusion fluxes depend on the polarity of the ion species. This gives rise to charge separation and induces an electric field. To the best of our knowledge, despite being a direct consequence of the fundamental Stokes-Einstein equation, such an effect has never been described before.

To further evaluate S, ψ has to be determined by solving the Poisson equation. Along with Eq. (4), one finds to leading order in A

$$\partial_{\tilde{z}}^2 \Psi \approx \kappa^2 \sinh(\Psi). \tag{9}$$

The local Debye parameter is given by $\kappa = \sqrt{2e^2\nu^2 n/(\epsilon k_B T)}$. Note that since $T = T(x)$, $\Psi = \Psi(x)$ and $\kappa = \kappa(x)$ as well [we set $\kappa_r = (\kappa)_{|x=0}$, with $T = T_r$ and $n = n_r$ as a reference]. However, the modification of S_ψ caused by these dependences is of higher order in d_xT and can be neglected in most situations. The solution of (9) is formally identical to the one of the isothermal Poisson-Boltzmann (PB) equation. Within the Debye-Hückel (DH) approximation ($|\Psi| < 1$) it reads $\psi^{(\mathrm{DH})} = \zeta \cosh(\kappa z)/\cosh(\bar{\kappa})$, where $\bar{\kappa} = \kappa h$, and ζ is the ζ potential at the slipping plane of the wall. With this, the integrals in (7) and (8) can be evaluated, yielding

$$S_Q^{(\mathrm{DH})} = \frac{1}{T}\frac{\Delta Q}{2e\nu}\frac{1}{1+\frac{\bar{\zeta}^2}{4}\left[\frac{\tanh(\bar{\kappa})}{\bar{\kappa}}+\frac{1}{\cosh^2(\bar{\kappa})}\right]}, \tag{10}$$

and

$$S_\psi^{(\mathrm{DH})} = \frac{\zeta}{T}\frac{\tanh(\bar{\kappa})}{\bar{\kappa}}\frac{1+\frac{\bar{\zeta}^2}{2}\left[\frac{\tanh^2(\bar{\kappa})}{3}+\frac{1}{\cosh^2(\bar{\kappa})}\right]}{1+\frac{\bar{\zeta}^2}{4}\left[\frac{\tanh(\bar{\kappa})}{\bar{\kappa}}+\frac{1}{\cosh^2(\bar{\kappa})}\right]}, \tag{11}$$

with $\bar{\zeta} \equiv e\nu\zeta/(k_B T)$. According to (10) and for sufficiently small ζ, the effect of the EDL on the Soret voltage is negligibly small. At constant ζ, for $\bar{\kappa} \to 0$ one has $S_\psi^{(\mathrm{DH})} \to \zeta/T$, whereas $S_\psi^{(\mathrm{DH})}$ vanishes for $\bar{\kappa} \to \infty$. Hence, the thermoelectric field induced by a temperature-dependent electrophoretic ion mobility is a confinement effect and dominant in charged, narrow channels.

In Fig. 2, the Seebeck coefficient S_ψ, nondimensionalized by ζ/T, is plotted as a function of $\bar{\kappa}_r$, while $\zeta = [15, 75, 125] \times 10^{-3}$ V. The solutions according to the DH approximation are compared to those based on numerical evaluations of Eq. (9) ([20], Sec. 6). With

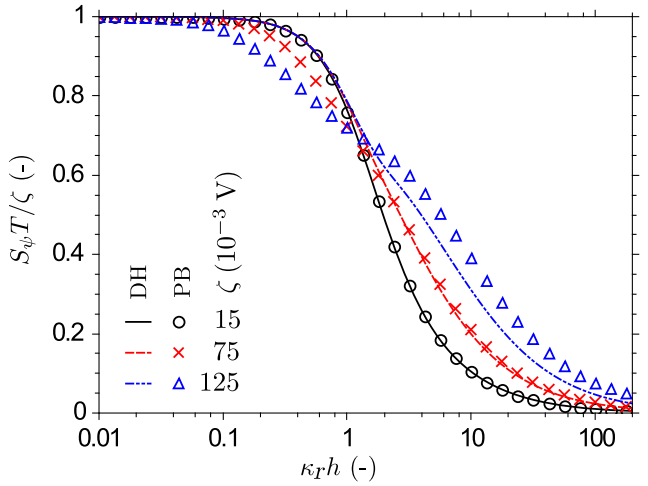

FIG. 2. Seebeck coefficient S_ψ relative to ζ/T and as a function of the nominal Debye parameter $\bar{\kappa}_r = \kappa_r h$. Results based on the Debye-Hückel (DH) approximation [lines without symbols, computed by (11)], are compared to solutions based on a numerical evaluation (PB, Poisson-Boltzmann) of (9) (lines with symbols). All data were calculated for $T = 298$ K.

increasing $\bar{\kappa}_r$, all curves continuously decrease from unity to zero. The PB solutions and the DH approximation are indistinguishable for $\zeta = 15 \times 10^{-3}$ V and almost identical for $\zeta = 75 \times 10^{-3}$ V if $\bar{\kappa}_r > 2$. If $\bar{\kappa}_r \lesssim 2$ while $\zeta = 75 \times 10^{-3}$ V, the DH approximation overpredicts S_ψ. This occurs also for $\zeta = 125 \times 10^{-3}$ V, whereas in that case for $\bar{\kappa}_r \gtrsim 2$ S_ψ is underpredicted. All data shown were evaluated at $T = T_r = 298$ K. Corresponding calculations at $T = 308$ K (using $\Pi/T = 5 \times 10^{-3}$ K^{-1} [35–37] and $d_T\epsilon/\epsilon = -5.1 \times 10^{-3}$ K [38]) to estimate the magnitude of possible nonlinear effects due to $\bar{\kappa} = \bar{\kappa}(T)$ gave practically indistinguishable results (not shown).

The NPE treat the ions as point charges, so that the effects of the finite ion size [39] and ion-ion correlations on steric and Coulombic interactions [40] are neglected. This is permissible for ion concentrations and ζ potentials not significantly exceeding $n_r = 0.01$ M and $\zeta = 125 \times 10^{-3}$ V [41]. The effect under study is at its maximum for $\bar{\kappa} \to 0$. In this limit the ion cloud does not completely screen the surface charge; i.e., ψ is nonvanishing at the center of the channel. While for sufficiently wide channels the Gouy-Chapman (GC) equation implies the equivalency of a constant ζ potential and a constant value of q [42], this does not hold for channels with pronounced EDL overlap [43]. In this case, the variation of the electrokinetic characteristics of a system as a function of $\bar{\kappa}_r$ may be different depending on whether a constant value of ζ or of q is imposed. Furthermore, the constituting equations of the PB model are derived in the framework of a first-order expansion in A. Especially the validity of (4) in case of overlapping EDLs has to be confirmed, since the reference concentrations at $\psi = 0$, $n_{k,0}$, can no longer refer to a location inside the channel. Such issues can be avoided by a

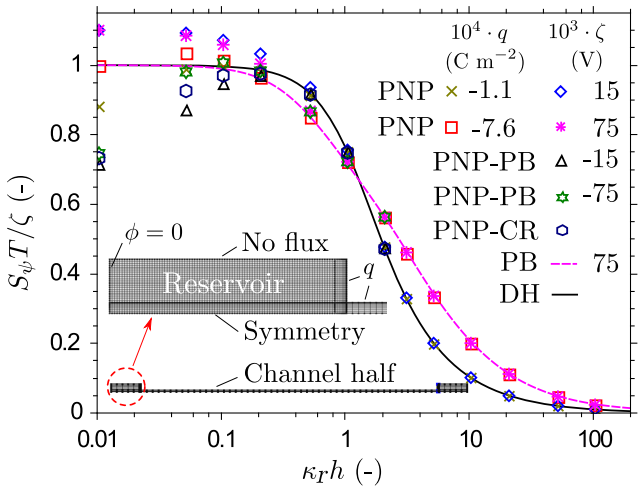

FIG. 3. Seebeck coefficient S_ψ relative to ζ/T and as a function of the nominal Debye parameter $\bar{\kappa}_r = \kappa_r h$. The data points are obtained from a full numerical simulation of the Poisson equation and the Nernst-Planck equation (PNP), without relying on (4). Either the surface charge density q or the ζ potential is held constant. The PNP model is compared with the Debye-Hückel (DH) approximation (11) as well as with the Poisson-Boltzmann (PB) model, which is based on a numerical evaluation of (9). For selected cases (PNP-PB), q imposed in the PNP simulation as a boundary condition was predetermined for a given $\bar{\kappa}_r$ from an analytical solution of (9), where ζ was set either to -15 or -75×10^{-3} V. For a pH value of 4, the PNP simulation was also combined with a temperature-dependent charge regulation model (PNP-CR), which is detailed in the Supplemental Material ([20], Sec. 9). The temperature was set to $T = 298$ K.

(numerically solved) model solely based on the coupled Poisson- and Nernst-Planck (PNP) equations, without relying on (4). In Fig. 3, the results of such simulations for the given system are shown. The computations ([20], Sec. 7) followed the basic strategy outlined in Refs. [43,44] and were conducted using COMSOL MULTIPHYSICS 4.3a [45]. While varying $\bar{\kappa}_r$, either a constant ζ potential ($\zeta = [15, 75] \times 10^{-3}$ V) or a constant surface charge density ($q = [-1.1, -7.6] \times 10^{-4}$ C m^{-2}) was imposed along the channel walls, where the mapping between ζ and q is provided by the GC model ([20], Sec. 7). Given the negligible extent of advection, the Navier-Stokes equations were not included in the model.

In Fig. 3 the (relative) Seebeck coefficient $S_\psi T/\zeta$ is shown as a function of $\bar{\kappa}_r$. For the numerical simulations (depicted as symbols), the variation of $\bar{\kappa}_r$ was achieved by a variation of h, with the nominal EDL thickness being held constant at $\kappa_r^{-1} \approx 10^{-7}$ m. For low ζ or q, the numerical results are compared with the DH approximation, while for more strongly charged walls they are compared with the PB model. For $\bar{\kappa}_r > 0.5$, the PNP solutions fully agree with the corresponding (quasi)analytical solutions (DH or PB). From the PNP simulations conducted at constant q, it follows that the surface charge is almost completely screened if h is at least twice the nominal EDL thickness.

The PNP simulations of the cases with overlapping EDLs ($0.01 \leq \bar{\kappa}_r \leq 2$) were repeated by imposing q at the charged walls, with its value—for given ζ and $\bar{\kappa}_r$—being individually precalculated by the analytical solution of the PB equation (9) [46] rather than using the GC model ([20], Sec. 8). For $0.2 \leq \bar{\kappa}_r \leq 2$ at $\zeta = -15$ or -75×10^{-3} V, the corresponding results (see Fig. 3) agree well with those where a constant ζ potential is imposed directly. For decreasing $\bar{\kappa}_r$ below 0.2, the PNP model increasingly deviates from the DH and PB models for any considered ζ potential or q. This is likely caused by an insufficient length of the channel in the computational domain, but could not be resolved with the available computational resources. From the PNP simulations it was also found that the Soret voltage under confinement, expressed by (7), deviates from its bulk value $S_Q^{(\infty)}$ by not more than 1% for any channel width.

The invariance of either the ζ potential or q along the channel wall does not necessarily hold for a nonisothermal channel, and both parameters might be a function of temperature [47]. Such questions can be addressed by detailing the surface charge formation process [48,49]. For a silica channel with its surface charge being mainly formed by the dissociation of silanol groups, corresponding results are included in Fig. 3. For a pH value of 4, the model was calibrated with experimental data available for NaCl as electrolyte ([20], Sec. 9). It is apparent that the results using the (temperature-dependent) charge regulation model follow closely those of the other approaches. Consequently, the thermoelectricity described by (8) [and in the DH limit by (11)], being the main result of this work, is remarkably robust for values of $\bar{\kappa}_r$ larger than about 0.2.

The prediction of S_ψ is firmly linked to the particular expression of the electrophoretic ion mobility in the form of the Einstein-Smoluchowski equation, which is the simplest form of a fluctuation-dissipation relation under infinite dilution. It was derived under the assumption of isothermal conditions [50], and its use in nonisothermal systems of low ionic strength is acceptable only if the momentum relaxation time of an ion is much smaller than the time the particle takes to experience a temperature change [51]. Herein, the ratio between these characteristic time scales is $O(10^{-8})$ ([20], Sec. 10). For systems of higher ionic strength and complex electrolyte solutions, the electrophoretic ion mobility might be itself a nontrivial function of temperature [52], which is beyond the scope of the present work.

Our results indicate that the thermoelectric voltage of dilute electrolytes in confined geometry may be quite different from its bulk counterpart. While the presence of the latter is intrinsically linked to different thermophoretic mobilities of the ion species alone, the former may be present even if the heats of transport of each ion species are identical ($\Delta Q = 0$) or very small. In this case, the thermoelectric voltage under confinement is solely proportional to the ζ potential or surface charge density of the channel and

reaches its maximum in the limit of $\bar{\kappa}_r \to 0$. For narrow, highly charged channels and within the validity range of the presented theory, such thermovoltages might be up to 30 times larger than the values of the conventional Soret voltage being typical for simple monovalent electrolytes in the bulk ([20], Sec. 11). Our findings can be used as a novel method to determine the ζ potential of nanochannels and biological ion channels, while also being of interest for the design of novel small-scale heat exergy (i.e., availability) recovery devices. Even though the presented theory is strictly valid only for domains of a small aspect ratio, the underlying mechanism may still have an impact on the thermophoretic motion of larger, charge-stabilized particles [53,54] and biological molecules [55].

*dietzel@csi.tu-darmstadt.de

[1] N. S. Hudak and G. G. Amatucci, J. Appl. Phys. **103**, 101301 (2008), and references therein.
[2] A. W. van Herwaarden and P. M. Sarro, Sens. Actuators **10**, 321 (1986).
[3] S. B. Riffat and X. Ma, Appl. Therm. Eng. **23**, 913 (2003).
[4] L. E. Bell, Science **321**, 1457 (2008).
[5] A. Shakouri, Annu. Rev. Mater. Res. **41**, 399 (2011).
[6] D. G. Cahill, W. K. Ford, K. E. Goodson, G. D. Mahan, A. Majumdar, H. J. Maris, R. Merlin, and S. R. Phillpot, J. Appl. Phys. **93**, 793 (2003).
[7] H. J. Goldsmid, in *Introduction to Thermoelectricity*, Springer Series in Materials Science Vol. 1, edited by R. Hull, J. Parisi, J. R. M. Osgood, and H. Warlimont (Springer, Heidelberg, 2010).
[8] G. Guthrie, J. N. Wilson, and V. Schomaker, J. Chem. Phys. **17**, 310 (1949).
[9] A. Würger, Rep. Prog. Phys. **73**, 126601 (2010).
[10] G. J. Hills, P. W. M. Jacobs, and N. LakshimiNarayanaiah, Nature (London) **179**, 96 (1957).
[11] M. Tasaka, S. Morita, and M. Nagasawa, J. Phys. Chem. **69**, 4191 (1965).
[12] M. Tasaka, Pure Appl. Chem. **58**, 1637 (1986).
[13] F. S. Gaeta, E. Ascolese, U. Bencivenga, J. M. O. de Zárate, N. Pagliuca, G. Perna, S. Rossi, and D. G. Mita, J. Phys. Chem. **96**, 6342 (1992).
[14] R. B. Schoch, J. Han, and P. Renaud, Rev. Mod. Phys. **80**, 839 (2008).
[15] D. D. McKemy, Eur. J. Phys. **454**, 777 (2007).
[16] G. Reid and M.-L. Flonta, Nature (London) **413**, 480 (2001).
[17] F. Viana, E. de la Peña, and C. Belmonte, Nat. Neurosci. **5**, 254 (2002).
[18] K. D. Sandbakk, A. Bentien, and S. Kjelstrup, J. Membr. Sci. **434**, 10 (2013).
[19] B. Xu, L. Liu, H. Limb, Y. Qiao, and X. Chen, Nano Energy **1**, 805 (2012).
[20] See Supplemental Material at http://link.aps.org/supplemental/10.1103/PhysRevLett.116.225901, which includes Refs. [21–32], for derivation details.
[21] B. Derjaguin, N. Churaev, and V. Muller, in *Surface Forces* (Plenum, New York, 1987).
[22] D. R. Lide, in *CRC Handbook of Chemistry and Physics*, edited by D. R. Lide (CRC Press, Boca Raton, 2009).
[23] N. Takeyama and K. Nakashima, J. Phys. Soc. Jpn. **52**, 2699 (1983).
[24] A. Castellanos, in *Electrohydrodynamics*, edited by A. Castellanos (Springer, Wien, 1998).
[25] F. Baldessari and J. G. Santiago, J. Colloid Interface Sci. **325**, 526 (2008).
[26] T. Hiemstra, J. C. M. D. Wit, and W. H. V. Riemsdijk, J. Colloid Interface Sci. **133**, 105 (1989).
[27] P. Leroy, N. Devau, A. Revil, and M. Bizi, J. Colloid Interface Sci. **410**, 81 (2013).
[28] Y. V. Alekhin, M. P. Sidorova, L. I. Ivanova, and L. Z. Lakshtanov, Colloid J. USSR **46**, 1032 (1984).
[29] E. H. Oelkers and H. C. Helgeson, J. Solution Chem. **18**, 601 (1989).
[30] National Institute of Standards and Technology, http://webbook.nist.gov.
[31] Royal Society of Chemistry, http://www.chemspider.com.
[32] G. Falasco, M. V. Gnann, and K. Kroy, arXiv:1406.2116v1.
[33] J. C. Fair and J. F. Osterle, J. Chem. Phys. **54**, 3307 (1971).
[34] V. Sasidhar and E. Ruckenstein, J. Colloid Interface Sci. **85**, 332 (1982).
[35] P. N. Snowdon and J. C. R. Turner, Trans. Faraday Soc. **56**, 1812 (1960).
[36] J. N. Agar and J. C. R. Turner, Proc. R. Soc. A **255**, 307 (1960).
[37] P. N. Snowdon and J. C. R. Turner, Trans. Faraday Soc. **56**, 1409 (1960).
[38] R. Buchner, G. T. Hefter, and P. M. May, J. Phys. Chem. A **103**, 1 (1999).
[39] F. Tessier and G. W. Slater, Electrophoresis **27**, 686 (2006), and references therein.
[40] M. Z. Bazant, M. S. Kilic, B. D. Storey, and A. Ajdari, Adv. Colloid Interface Sci. **152**, 48 (2009), and references therein.
[41] J. Cervera, P. Ramírez, J. A. Mantanares, and S. Mafé, Microfluid. Nanofluid. **9**, 41 (2010).
[42] W. B. Russel, D. A. Saville, and W. R. Schowalter, in *Colloidal Dispersions* (Cambridge University Press, Cambridge, 1989).
[43] S. Movahed and D. Li, Electrophoresis **32**, 1259 (2011).
[44] H. Daguji, Y. Oka, T. Adachi, and K. Shirano, Electrochem. Comm. **8**, 1796 (2006).
[45] Comsol Multiphysics, COMSOL®, Inc., Göttingen, Germany, 2014.
[46] S. H. Behrens and M. Borkovec, Phys. Rev. E **60**, 7040 (1999).
[47] P. M. Reppert and F. D. Morgan, J. Geophys. Res. **108**, 2546 (2003).
[48] S. H. Behrens and D. G. Grier, J. Chem. Phys. **115**, 6716 (2001).
[49] A. Revil and P. W. J. Glover, Phys. Rev. B **55**, 1757 (1997).
[50] A. Einstein, Ann. Phys. (Berlin) **322**, 549 (1905).
[51] G. Stolovitzky, Phys. Lett. A **241**, 240 (1998).
[52] A. Rogacs and J. G. Santiago, Anal. Chem. **85**, 5103 (2013).
[53] M. Braibanti, D. Vigolo, and R. Piazza, Phys. Rev. Lett. **100**, 108303 (2008).
[54] A. Majee and A. Würger, Phys. Rev. E **83**, 061403 (2011).
[55] M. Reichl, M. Herzog, A. Götz, and D. Braun, Phys. Rev. Lett. **112**, 198101 (2014).